close to the observed value 29sin(ℓ + 241°) mas.

23. We thank the Mars Pathfinder project team for their enthusiasm and assistance in acquiring and understanding the tracking measurements; R. Wimberly for recovery of the Viking lander Doppler data; and J. Williams and an anonymous referee for helpful suggestions. The research described in this paper was carried out by the Jet Propulsion Laboratory, California Institute of Technology, under a contract with NASA.

11 September 1997; accepted 5 November 1997

The Mars Pathfinder Atmospheric Structure Investigation/Meteorology (ASI/MET) Experiment

J. T. Schofield, J. R. Barnes, D. Crisp, R. M. Haberle, S. Larsen, J. A. Magalhães, J. R. Murphy, A. Seiff, G. Wilson

The Mars Pathfinder atmospheric structure investigation/meteorology (ASI/MET) experiment measured the vertical density, pressure, and temperature structure of the martian atmosphere from the surface to 160 km, and monitored surface meteorology and climate for 83 sols (1 sol = 1 martian day = 24.7 hours). The atmospheric structure and the weather record are similar to those observed by the Viking 1 lander (VL-1) at the same latitude, altitude, and season 21 years ago, but there are differences related to diurnal effects and the surface properties of the landing site. These include a cold nighttime upper atmosphere; atmospheric temperatures that are 10 to 12 degrees kelvin warmer near the surface; light slope-controlled winds; and dust devils, identified by their pressure, wind, and temperature signatures. The results are consistent with the warm, moderately dusty atmosphere seen by VL-1.

The ASI/MET experiment consists of a suite of sensors designed to measure the vertical structure of the atmosphere during entry, descent, and landing (EDL) and to study martian surface meteorology and climate for the duration of the Pathfinder mission (*1*, *2*). In situ vertical structure measurements were made only twice by the Viking entry vehicles (*3*), both during the daytime. In addition to adding a third profile, ASI/MET provides the first nighttime observation, giving information about the diurnal variation of vertical structure, particularly in the upper atmosphere, which is inaccessible to existing remote-sensing techniques. Both Viking landers obtained records of atmospheric pressure, temperature, and wind velocity at the surface that extended over several Mars years. More recent Earth-based, disk-averaged microwave observations have been interpreted to indicate episodic cooling of the martian lower atmosphere by about 20 K relative to the conditions observed during the Viking missions (*4*). By continuing the Viking record after 21 years, ASI/MET results are able to determine whether martian meteorology and climate have changed or remained stable in the late northern summer. Improved measurement sensitivity and temporal resolution (*2*) also reveal phenomena not seen by Viking and, together with temperature measurements at three levels, give better information on the exchange of heat and momentum between the atmosphere and the surface.

The ASI/MET experiment combined accelerometer and MET instruments (*2*). The accelerometer instrument contained science and engineering accelerometers that each monitored accelerations along three orthogonal axes. In each axis, the maximum sensitivity was 20 μm/s^2 [2 × 10^{-6} Earth gravities (*g*)], and the accelerations expected during EDL were covered by commandable measurement ranges of 16mg, 800mg, and 40*g* full-scale. The MET instrument consisted of pressure, temperature, and wind sensors. Pressure was measured through a 1-m inlet tube that was exposed to the atmosphere during parachute descent as well as after landing (*1*, *2*). The pressure measurements have a maximum sensitivity of 0.25 μbar, which is more than a factor of 100 better than that available to the Viking landers (*5*). All the MET temperature and wind sensors are mounted on a mast 1.1 m high, deployed at the end of a lander petal to isolate it from spacecraft thermal contamination (*1*, *2*). Atmospheric temperature was measured by four thermocouples: one designed to measure temperature during parachute descent and three designed for surface boundary layer measurements 25, 50, and 100 cm above the base of the mast. All four thermocouples have time constants of 1 to 2 s and sensitivities of 0.01 K. Wind was measured by a six-segment hot-wire sensor at the top of the mast, 1.1 m above the mast base. The wires are heated by a current passed in series through all six segments, and the temperature differences between low and high current modes for each segment are used to determine wind speed and direction.

The accelerometer and MET instruments recorded data continuously throughout EDL until about 1 min after impact at about 03:00 local solar time (LST). Regular surface pressure, temperature, and wind measurements by the MET instrument began about 4 hours after impact at 07:00 LST on sol 1 (1 sol = 1 martian day = 24.7 hours), and the MET mast was deployed at 13:30 LST.

The science accelerometer detected the upper atmosphere 160 km above the landing site when the entry vehicle had a velocity of 7.4 km/s relative to the atmosphere and a flight path angle 14.8° below the local horizontal. 1.5 min later, the entry vehicle experienced a peak deceleration of 15.9*g* at an altitude of 33 km. After 3 min (9 km) the parachute deployed, and at 3.4 min (7.4 km) the heat shield separated from the lander, allowing the pressure sensor to begin unobstructed measurements of the atmosphere. The inflation of shock-absorbing airbags at 5.1 min (0.3 km) terminated the unobstructed pressure measurements, and descent rocket firing at 5.2 min (0.1 km) ended the direct measurement of aerodynamic decelerations. The first impact of the probe with the martian surface occurred 5.3 min after it entered the atmosphere. In the first minute after impact, the lander bounced 15 times and pressure sensor data indicated that it rolled 10 m vertically downhill. It came to rest about a minute later at a site 3389.7 km from the center of mass of Mars (*6*). Surface acceleration measurements of 3.716 m/s^2 agree with values of 3.717 m/s^2 calculated for the lander location and height (*7*), providing a verification of accelerometer gain calibration.

Because the engineering accelerometers were used to control parachute deployment and remained in their least sensitive 40*g* scale, atmospheric profiles were derived from science accelerometer data only, which were logged at 32 Hz throughout EDL. MET pressure and temperature data were collected at 2 Hz during the parachute

J. T. Schofield and D. Crisp, Jet Propulsion Laboratory, California Institute of Technology, 4800 Oak Grove Drive, Pasadena, CA 91109, USA.
J. R. Barnes, College of Oceanic and Atmospheric Sciences, Oregon State University, Corvallis, OR 97331, USA.
R. M. Haberle, Ames Research Center, Moffett Field, CA 94035–1000, USA.
S. Larsen, Wind Energy and Atmospheric Physics, Risoe National Laboratory, AMV-125, Post Office Box 49, Roskilde, Denmark DK-4000.
J. A. Magalhães, J. R. Murphy, A. Seiff, San Jose State University Foundation, San Jose, CA, and Ames Research Center, Moffett Field, CA 94035–1000, USA.
G. Wilson, Arizona State University, Tempe, AZ, and Ames Research Center, Moffett Field, CA 94035–1000, USA.

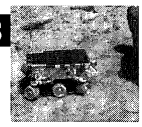

descent and landing phases of EDL. However, spacecraft design constraints did not allow the descent temperature sensor to be exposed to the free flow around the lander, so that direct atmospheric temperature measurements were not possible (*2*, *8*).

For the 30-day primary landed mission, 51 equally spaced MET measurement sessions were made each day to monitor the atmospheric diurnal cycle and synoptic (day-to-day) variations. These 3-min sessions sampled the atmosphere at 4-s intervals and were interspersed with 15-min and 1-hour sessions of 1-s sampling to monitor the surface boundary layer. The boundary layer sessions were repeated as frequently as allowed by data volume, in a pattern that sampled all local times of day as rapidly as possible. Finally, on sol 25, a 24-hour session was executed that sampled science data continuously at 4-s intervals for a complete daily cycle. The continuous MET observations desired during the primary mission were interrupted by spacecraft computer resets. One of these resets was associated with errors in MET software, and the measurements were limited to the nighttime from sols 12 to 17, until the errors were corrected.

Entry, descent, and landing. Atmospheric density, pressure, and temperature profiles were derived from ASI/MET deceleration measurements during Pathfinder EDL and compared with VL-1 results (Figs. 1 and 2). The mean solar forcing of the martian atmosphere at the time of the Pathfinder and VL-1 profiles was similar. Solar longitudes (L_s) of 98° (VL-1) and 142° (Pathfinder) correspond to a seasonal difference from mid- to late summer and to a smaller Mars-sun distance at the time of the Pathfinder profile. Solar activity, as measured by sunspot counts, was near-minimum for both profiles, the lower atmosphere had comparable amounts of dust (*9*), and the two landings were at similar latitudes and longitudes on Mars. However, the different time of day (03:00 LST for Pathfinder versus 16:15 LST for VL-1) and the 21 years separating the two entry profiles suggest that diurnal and secular effects could be important in understanding their differences.

For an entry vehicle, atmospheric density is directly related to aerodynamic deceleration, velocity relative to the atmosphere, and aerodynamic characteristics (*2*). Deceleration was measured directly; velocity and position can be reconstructed by integrating the equations of motion using the observed decelerations and an initial velocity and position; and Pathfinder entry vehicle aerodynamic characteristics are known from computational aerodynamic simulations and laboratory experiments.

Atmospheric densities measured by Pathfinder varied from $\sim 5 \times 10^{-11}$ kg/m^3 at the threshold of detection to 8×10^{-3} kg/m^3 immediately before parachute release at 9 km (Fig. 1). From 160 to 90 km, densities range from a factor of 5 lower than VL-1 values near and above 120 km to a factor of 2.5 lower near 90 km. The increase in density between 90 and 80 km, which corresponds to a deep temperature minimum (Fig. 2), raises the Pathfinder densities at lower altitudes to values slightly lower than VL-1 densities. The lower values of density, and therefore pressure, encountered by Pathfinder below 30 km are generally consistent with the lower overall mass and surface pressure of the martian atmosphere at the time of the Pathfinder landing (*10*). The decreased surface pressure results from the annual variation in atmospheric mass caused by condensation and sublimation from the polar caps (*11*).

The martian thermosphere, where temperature increases rapidly with altitude because of heating by solar extreme ultraviolet radiation, is evident above 125 km in the Pathfinder profile (Fig. 2). Although the uncertainties in the derived temperatures at these altitudes are large, it appears that Pathfinder temperatures are close to or slightly higher than those measured by VL-1.

From 65 to 125 km, observed temperatures were, on average, 20 K lower than those observed by VL-1 (Fig. 2). This contrast is responsible for the lower Pathfinder densities above 90 km. Because radiative time constants reach a minimum in this altitude range, a large response to diurnal forcing is a likely explanation for this difference (*12*). The temperature minimum of 92 K at 80 km is the lowest temperature ever measured in the martian atmosphere and may result from the superposition of waves, such as thermal tides, on the overall nighttime cooling. Tides propagate from the lower atmosphere with amplitudes that

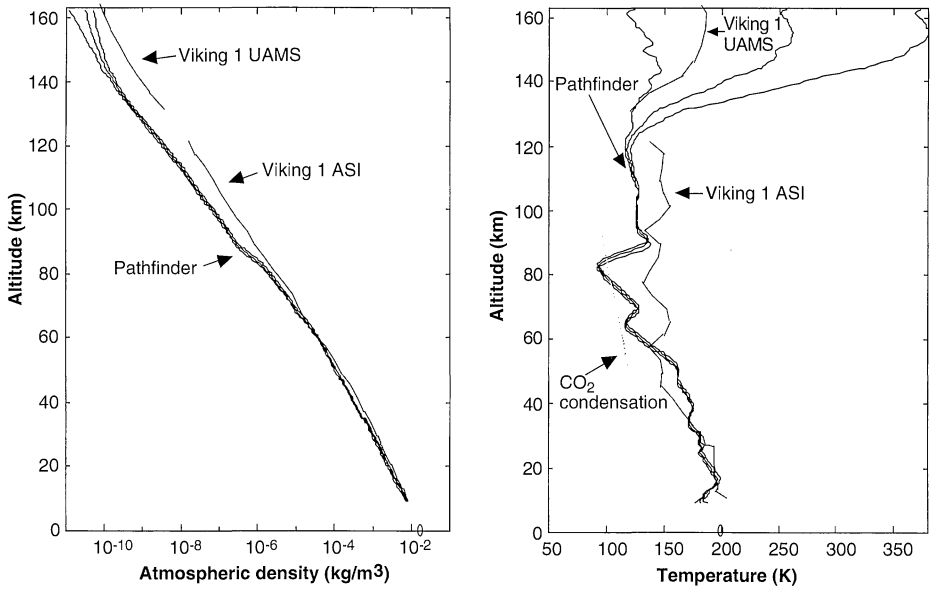

Fig. 1 (left). The atmospheric density profile derived from ASI/MET. The solid lines give the mean atmospheric density profile derived from the accelerometer data and profiles reflecting $\pm 2\sigma$ uncertainties in density based on uncertainties in the entry velocity and the finite digital resolution of the instrument. Errors in aerodynamic characteristics are not included but are not expected to change the error envelopes substantially. Further work with the accelerometer and pressure data will allow us to extend the density profile down to the surface, where the MET observations of pressure and temperature indicate an atmospheric density of 1.76×10^{-2} kg/m^3, marked by an oval on the *x* axis of the figure. Results from the VL-1 atmospheric structure instrument (ASI) (*2*, *3*) and the Viking 1 upper atmosphere mass spectrometer (UAMS) are also plotted for comparison (*2*, *3*). **Fig. 2 (right).** The atmospheric temperature profile derived from the Pathfinder atmospheric density profile. Temperature profiles corresponding to the nominal and $\pm 2\sigma$ density profiles of Fig. 1 are represented by solid lines. The hydrostatic equation is integrated to derive a pressure profile from the density profile, and temperature is calculated from density and pressure with the use of the ideal gas law. To begin the integration, an upper boundary temperature is determined from the density scale height at the upper boundary. Uncertainties in this temperature affect the derived profiles significantly only above 125 km. In order to derive temperatures, we have constructed a molecular weight versus atmospheric density model based on the results of the Viking UAMS (*29*). At present, we have no way of quantifying the accuracy of this model, which influences temperature above 120 km. At lower altitudes, the martian atmosphere is well mixed, with a constant molecular weight of 43.49. Temperature profiles from the VL-1 ASI and UAMS experiments (*2*, *3*), the CO_2 condensation temperature profile, and the surface temperature measured by the Pathfinder MET instrument (circle) are also shown for comparison.

increase with altitude.

At 80 km, the Pathfinder temperature profile is lower than the CO_2 condensation temperature (Fig. 2). The lower temperature may result from supercooling or from inaccuracies in the vapor pressure curve for CO_2 (*13*), but it is possible that CO_2 could be condensing at these levels to form high-altitude clouds. Observations by the imager for the Mars Pathfinder (IMP) of sky brightening well before the expected start of dawn may indicate the presence of such clouds, although the substantial morning clouds identified in images of the eastern horizon before sunrise are almost certainly water clouds formed at much lower levels (*9*).

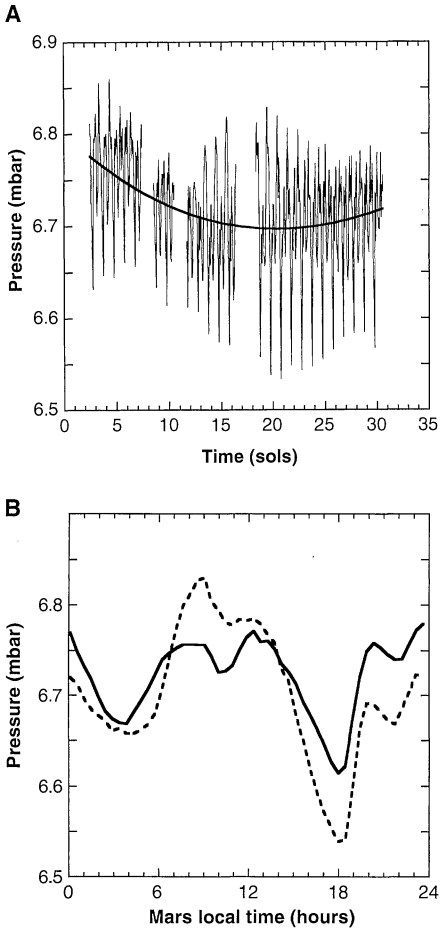

Fig. 3. (**A**) Time-averaged surface pressures measured by the MET instrument over the first 30 sols of the Pathfinder landed mission. The averages are primarily over the 3-min default measurement sessions, of which there are nominally 51 per sol; and the resulting points have been connected with straight lines, except for sols 12 through 15, where cubic spline interpolation has been used to fill data gaps of about 8 hours in length. MET operation was restricted to nighttime observations during this period to prevent spacecraft resets associated with MET data collection. The major gaps in the data set at sols 1, 8, 11, and 17 are caused by various spacecraft software reset and downlink problems. After sol 17, the reset problems associated with MET were corrected, and continuous sampling was resumed. The long-term trend in pressure is represented by a third-order polynomial fit to the data (solid curve). (**B**) Diurnal pressure cycles for sols 9 (solid line) and 19 (dashed line), illustrating the observed day-to-day changes in the diurnal pressure cycle and allowing details of the daily pressure variation to be seen more clearly.

Below 60 km, temperatures measured by Pathfinder are higher than those measured by VL-1 down to 35 km and are similar or slightly lower at lower altitudes down to 16.5 km (Fig. 2). These differences are consistent with minor variability in dust content and are also within the amplitudes expected from vertically propagating atmospheric waves such as tides (*10*). In view of the similar solar forcing, it is not surprising that the Pathfinder and VL-1 profiles are comparable in the lower atmosphere. However, Earth-based, disk-averaged microwave observations over the past 10 to 15 years have been used to suggest that the martian lower atmosphere undergoes episodes of cooling, which are characterized by reduced solar-absorbing dust content and 20 K lower temperatures relative to the conditions observed during the Viking mission (*4*). The Pathfinder entry profile shows no evidence for substantial cooling of the lower atmosphere (Fig. 2), although microwave profiles obtained before and after landing suggested that a cool atmosphere would be found (*14*). Furthermore, IMP observations yield atmospheric dust opacities of 0.5 (*9*), which are comparable to those found by VL-1 at the same season. These opacities are consistent with our temperature profile observations. Finally, it is unlikely that Pathfinder entered a locally dusty and anomalously warm region, as dust opacities remained stable throughout the 30-day primary mission (*9*).

Below 16.5 km a strong thermal inversion is present in the Pathfinder data, where temperature decreases from 200 to 181 K at 10 km (Fig. 2). This inversion is at too high an altitude to be the strong thermal inversion in the lowest few kilometers of the nighttime diurnal thermal boundary layer on Mars predicted by radiative-convective models and one-dimensional dynamical boundary layer models (*15*, *16*). At the base of the Pathfinder profile, temperature appears to increase with decreasing altitude again and can easily achieve the observed surface temperature, including predicted near-surface thermal inversions, without exceeding the adiabatic lapse rate.

The temperature minimum in the 10-km inversion is well below the condensation temperature of water vapor in the martian atmosphere, assuming that the 10 precipitable micrometers of water derived from IMP measurements are uniformly mixed (*9*). This inversion may mark the altitude of clouds seen in IMP images before sunrise (*9*) and near the low-latitude morning terminator in Hubble Space Telescope images (*17*), although the height of these clouds is not well known. After sunrise, the clouds burned off rapidly, and the inversion may have disappeared. What triggered the formation of a strong temperature inversion is not known, but possible mechanisms include the horizontal advection of cooler air at 10 km and vertically propagating finite-amplitude gravity waves excited by surface topography in the strongly stratified near-surface nighttime boundary layer (*18*). Once clouds formed, thermal emission from the cloud tops could have enhanced the intensity of the inversion at night.

Measurements made after landing. The pressure, temperature, and wind velocity data acquired by ASI/MET during the landed mission allow the variability of the martian atmosphere at the Ares Vallis landing site to be studied during the midsummer season on short, daily, synoptic (day-to-day), and seasonal time scales. This reveals not only the local properties of the atmosphere and its interaction with the surface but also more global information on atmospheric dust loading, circulation, and the seasonal CO_2 cycle. Comparisons with VL-1 data taken at the same time of year can be used to identify longer-term climate changes.

Pressure data. During sols 1 through 30, surface pressure at the landing site underwent substantial daily variations of 0.2 to 0.3 mbar, which were associated primarily with the large thermal tides in the thin martian atmosphere (*11*) (Fig. 3A). Daily pressure cycles were characterized by a strong semidiurnal oscillation, with two minima and two maxima per sol, together with diurnal and higher-order components, although there was considerable day-to-day variability (Fig. 3B). The presence of a large semidiurnal tidal oscillation is indicative of atmospheric dustiness over broad regions of Mars and over an altitude range of at least 10 to 20 km (*19*).

A long-term trend in daily mean pressure was also seen. A third-order polynomial fit to the data shows that mean pressure fell slowly at the beginning of the period and rose at the end, with a minimum just under 6.7 mbar near sol 20 ($L_s \sim 153°$) (Fig. 3A). This time corresponds to the annual deep minimum in the seasonal pressure cycle associated with CO_2 condensation and sublimation in the polar regions of Mars and was seen previously by the Viking landers (*11*).

The ASI/MET pressure sensor detected a variety of pressure variations on relatively short time scales. These ranged from seconds to hours and had magnitudes of 1 to 50 μbar. The shorter time-scale variations

(<10 to 15 min) appear to be correlated with wind and temperature fluctuations and tend to be largest during late morning and early afternoon, when the boundary layer is most turbulent. The most dramatic pressure features were minima of 10 to 50 μbar, usually less than a minute in duration, associated with vortices (dust devils) passing over the lander. A particularly good example was seen during the continuous sampling of sol 25.

Temperature data. In common with the single-level observations made by VL-1 at the same season, the diurnal temperature variations at the three Pathfinder levels repeat from day to day with a high degree of consistency. The diurnal cycle was sampled particularly well on sol 25 (Fig. 4). For the top mast thermocouple, a typical maximum temperature was 263 K at 14:15 LST and a typical minimum was 197 K at 05:15 LST, shortly before sunrise. Because of the low density of the martian atmosphere, near-surface atmospheric temperatures are influenced by the surface temperature cycle, which is driven by solar heating during the day and infrared cooling at night. For this reason, diurnal temperature extremes at the bottom of the mast exceeded those at the top (Fig. 4). Temperatures at the top of the mast (1.1 m) were greater by 10 K during the day and 12 K at night than those seen at 1.6 m by VL-1, probably because of the lower albedo and greater thermal inertia of the surface at the Pathfinder landing site.

The diurnal variation of the vertical temperature gradient was also consistent from day to day. At sunrise, the atmosphere is typically stably stratified, and cool dense air lies near the surface (Fig. 5). As the surface warms, the air mass is heated from below. By about 06:30 LST, all three mast temperatures are about equal, indicating that the near-surface atmosphere is neutrally stable, because isothermal and adiabatic lapse rates are indistinguishable over a vertical range of 75 cm. By 07:30 LST, ground heating exceeds the ability of the atmosphere to transfer surface heating by conduction, the temperature gradient reverses, the atmosphere becomes unstable, and convection begins. Turbulent mixing carries heat from the surface and is revealed by large rapid temperature fluctuations of up to 15 to 20 K observed during the remainder of the morning and early afternoon. Later in the afternoon, the surface cools and turbulent mixing diminishes (Fig. 4). By 16:45 LST, the thermal profile is neutral and what surface winds are observed convect heat quickly. Shortly afterward, surface cooling causes the temperature gradient to invert, and the surface boundary layer becomes stably stratified for the duration of the night. Major nighttime temperature fluctuations are caused by downslope winds that disturb the surface boundary layer (Fig. 4).

Large near-surface temperature gradients of 10 to 15 K are probably a common feature of the martian daytime boundary layer. Because of low atmospheric densities, the convective heat flux is unable to cool the surface as efficiently as on Earth, where atmospheric fluxes typically remove 80 to 90% of the net surface radiative flux under convective conditions.

Wind data. The ASI/MET wind sensor measured wind speed and direction 1.1 m above the base of the mast. Accurate speed determination requires further calibration of the relation between wind speed, air temperature, and sensor hot wire overheat under Mars surface conditions and is not yet available. Here we discuss wind direction and approximate speed based on azimuthal variations of wire overheat, which are a function of both wind speed and direction.

For sols 1 to 30, wind direction generally rotated in a clockwise manner through all the points of the compass during the course of 1 sol (Fig. 6). This rotation was not uniform. Winds were consistently from the south in the late night and early morning hours and then rotated steadily through west, north, and east during the day. Over the 30-day period studied, nighttime wind direction was remarkably constant, but considerably more scatter was seen during the day (Fig. 6). The most anomalous wind variations were observed on sols 8 through 10, when northeasterly winds were absent from the daily cycle. A pronounced reduction in the daily variation of surface pressure was seen in the same time interval (Fig. 3).

The recurrent southerly wind from late evening through morning is consistent with a drainage flow down Ares Vallis, which rises to the south of the lander (*1*); and the northerly wind seen in the afternoon is indicative of flow up Ares Vallis. Although the clockwise rotation of the wind vector agrees with that expected from the westward-migrating classical diurnal thermal tide, the time-phasing of wind direction throughout the day does not. The classical tidal drive would generate a westerly maximum near 18:00 LST and a southerly maximum at about 12:00 LST. It therefore appears that local topography, or possibly nonclassical tides, are controlling the wind direction at the Pathfinder location during midsummer.

Winds measured at the VL-1 site at this same season 11 Mars years earlier (1976) were generally weak (<6 m/s), exhibited a time-averaged northwesterly direction, and were approximately upslope during the afternoon and downslope during the night and early morning. Increased wind speeds accompanied the increased pressure oscillations seen during the several sols surrounding L_s = 150 (*20*). If the winds are slope-driven at this

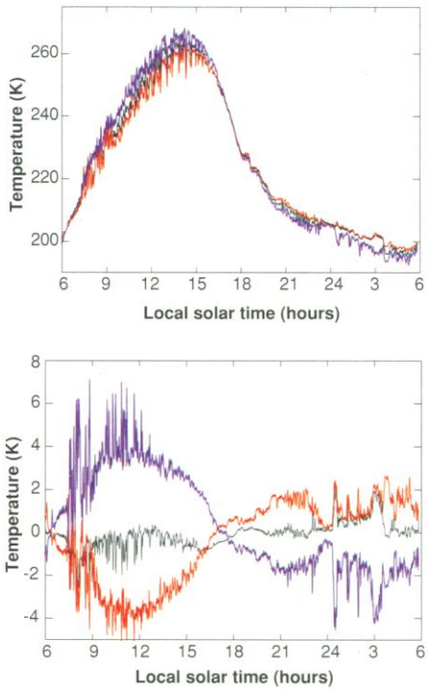

Fig. 4 (top). The diurnal variation of atmospheric temperature measured by the top (red), middle (black), and bottom (blue) mast thermocouples, from 06:00 LST on sol 25 to 06:00 LST on sol 26. These thermocouples are respectively 100, 50, and 25 cm above the plane of the lander solar panels. Temperatures are sampled continuously at 4-s intervals throughout this period, but the plots use 30-point (2-min) running means for clarity (this smoothing reduces the amplitude and frequency of the fluctuations that are present in the raw data). **Fig. 5 (bottom).** The data of Fig. 4 plotted as temperature deviations from the mean of all three thermocouples. Sampling times and data smoothing are identical to those of Fig. 4.

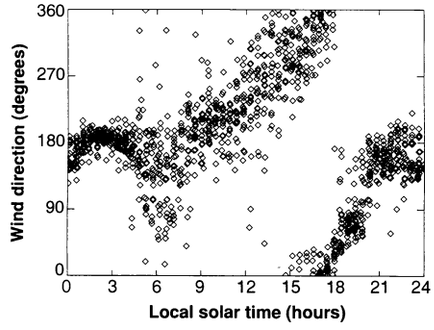

Fig. 6. Time-averaged wind direction measured by the MET instrument over the first 30 sols of the Pathfinder landed mission, plotted as a function of LST. Each point represents an average over a 3-min default measurement session. Wind direction is defined as follows: 0° and 360° (northerly), 90° (easterly), 180° (southerly), and 270° (westerly).

season, the differences between VL-1 and Pathfinder winds are expected to reflect differences in the magnitude and direction of the slope at the two sites. Finally, preliminary estimates suggest that wind speeds were comparable with or lower than those measured by VL-1 at the same time of year. Speeds were generally less than 5 to 10 m/s, except during the passage of dust devils, and were often less than 1 m/s in the morning hours. This may be consistent with the lower slope at the Pathfinder site.

Synoptic and seasonal variations. Synoptic and seasonal variability in the martian atmosphere at the Ares Vallis landing site are seen most clearly in the pressure data (Fig. 3). In particular, the annual pressure cycle reached a minimum at about sol 20, corresponding to the greatest mass of the southern seasonal polar cap (*11*), although the precise timing of the pressure minimum can be up to 5 sols earlier and 1 sol later, depending on exactly how the pressure data are analyzed. The Pathfinder minimum appears to have occurred about 6 sols later than that seen during the first year at the VL-1 site (*21*), which seems to imply more or longer lasting CO_2 condensation on the south polar cap. Variations from year to year of at least several sols in the timing of the annual pressure minimum were observed by the two Viking landers (*22*).

Small synoptic variations in amplitude of less than 3 to 4 K in temperature and 20 to 30 μbar in pressure are present in the ASI/MET data, after diurnal fluctuations and longer term trends are removed. Variations of comparable magnitude were found in the VL-1 data for this season; the greatest variance was at relatively long (10- to 30-sol) periodicities (*21*, *23*). Missing data and the limited temporal extent of the available Pathfinder observations make the estimation of periodicities difficult. On the basis of the VL-1 data and pre-landing general circulation model predictions for the Pathfinder site, it is expected that synoptic variations of much larger amplitude will begin as the transition to the fall and winter weather regime takes place (*10*, *21*). There is evidence that this is beginning to happen at the end of the Pathfinder pressure record.

Thermal tides. For the first 30 days of the landed mission, the semidiurnal tide was the largest component of the daily variation in surface pressure (Fig. 7). Its amplitude is generally similar to that found by VL-1 and is consistent with a visible optical depth of global dust of order 0.5 (*19*). This value is comparable to that measured by the IMP (*9*). Given the long vertical wavelengths associated with the semidiurnal tide, its measured amplitudes further suggest that the dust was deeply distributed in the atmosphere and was not confined to a shallow layer near the surface. This inference is consistent with the dust scale height of about 13 km deduced from IMP measurements (*9*) and with our entry profiles, which show a relatively warm lower atmosphere below 60 km. However, as mentioned earlier, a deeply distributed global dust haze is not consistent with Earth-based microwave measurements for this same period (*14*).

The amplitude of the diurnal tide was smaller and more variable. On sols 5 and 9, normalized amplitudes were down to 0.002 (Fig. 7), which is more than a factor of 2 smaller than anything measured by Viking. The variation seen by Pathfinder is somewhat systematic in that diurnal amplitudes were low during the first 5 to 10 sols, gradually rose to values of around 0.010 by sol 20, then declined to rather low values again by sol 27. Phase also varied during this period, retarding during the first 15 sols then advancing during the last 15 sols. The amplitude of the diurnal tide is sensitive to the calibration of the pressure sensor, which is still preliminary. However, the time variation of amplitude and phase is relatively insensitive to calibration.

These variations in the diurnal tide suggest that it was modulated by interference effects between the sun-following westward tide and the topographically induced, resonantly enhanced, eastward traveling, diurnal kelvin mode (*19*, *20*, *24*). One possibility is that the interaction is between eastward and westward modes of comparable amplitude, where the eastward mode period is first slightly greater than and later slightly less than 1 sol. Alternatively, the eastward and westward modes could have similar periods, and amplitudes may vary with time. The modeling of this interaction may help to distinguish between these two possibilities.

Nighttime temperature inflections. ASI/MET temperature measurements show that, on average, atmospheric temperatures fall monotonically through the evening and night until sunrise. On most nights, however, the steady decline in temperature was interrupted by one or more inflections in the gradient, where the temperature fell less rapidly or even rose before resuming its downward trend. Striking features of this kind are seen in Fig. 4 at 18:15, 19:00, 20:40, and 03:05 LST and are particularly marked in top mast thermocouple temperatures.

Temperature inflections seen in the VL-1 temperature data set were attributed to radiative effects associated with the formation of ground fogs (*25*). At the Pathfinder landing site, temperatures are about 10 K warmer than those of VL-1 at night, and condensation is unlikely, given the 10 precipitable micrometers of water measured by the IMP (*9*). However, there was a positive correlation between increased wind speed and the observed thermocouple temperature inflections. Increased horizontal flow may have disturbed the strong temperature inversion that developed at night, bringing warmer air from aloft down to thermocouple heights through enhanced vertical mixing. After the nighttime warming episodes, temperatures fell rapidly in conjunction with substantial reductions in wind speed. The nighttime temperature inflections occurred in the presence of southerly winds and cannot be produced by thermal contamination from the body of the spacecraft, which is located to the northwest of the MET mast.

Dust devils. Short-term variations in measured surface pressure, wind velocity, and air temperature over periods of tens of seconds to minutes suggest that small-scale convective vortices passed through the

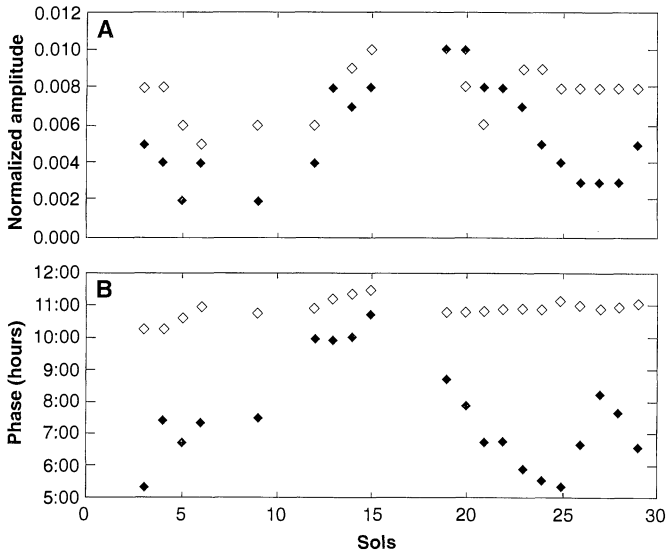

Fig. 7. (**A**) The amplitude of the diurnal (black diamonds) and semidiurnal (open diamonds) surface pressure tides for the first 30 sols of the Pathfinder landed mission. Amplitudes are normalized relative to the mean pressure for each day. (**B**) The phase, in LST, of the diurnal (black diamonds) and semidiurnal (open diamonds) surface pressure tides. Enough pressure data were collected to characterize the thermal tide on 20 sols. Pressure measurements from each of these sols were fitted with a cubic spline, from which 51 equally spaced intervals were sampled to define the tide.

Pathfinder lander site. During the passage of one of these features, pressure fell and recovered rapidly, accompanied by abrupt shifts in wind direction. These events, which we refer to as dust devils, are probably similar in character to features noted in the VL-1 and VL-2 meteorology data (*26*) and may have been seen by the Viking orbiter cameras (*27*). The narrow, well-defined pressure minimum is the most characteristic feature of these vortices, but it was not seen in the Viking lander pressure record because of poor resolution and coarse temporal sampling. There are currently no Pathfinder lander images to indicate whether the apparent vortices entrain dust, but the passage of a particularly large feature on sol 62 was correlated with a short-lived reduction of about 1.5% in the power generated by the Pathfinder solar panels.

A dust devil event at 14:15 LST on sol 25 has the characteristics of a clockwise-rotating vortex traveling toward the south-southeast (160°), with the vortex center passing west and south of the lander (Fig. 8). During this event, pressure fell 0.028 mbar in 24 s to a minimum, followed by a more rapid rise of 0.027 mbars in 8 s. The pressure minimum was accompanied by a local temperature maximum at all three thermocouple heights. These temperature maxima are themselves embedded in a pronounced temperature minimum, which extended 30 to 40 s before and after the pressure minimum. Wind direction rotated from northwesterly, which was the mean flow direction before the vortex arrived, through north to northeasterly in the 40 s preceding the pressure minimum, before shifting abruptly through northerly to westerly at and just after the pressure minimum. Wind direction slowly returned to north-northwesterly over the minutes following the pressure minimum. This pattern is consistent with a clockwise-rotating vortex embedded in an ambient flow that has a speed less than the vortex rotational speed (*26*).

Boundary layer results. The near-surface boundary layer of the martian atmosphere can be described by "universal" scaling laws involving dimensionless coefficients determined from measurements in Earth's atmosphere. The Viking and Pathfinder measurements provide us with an opportunity to test this universality by using measurements in another atmosphere. Although the martian atmosphere differs in many respects from our own, most of the universal relations are expected to be valid, based on the analysis of Viking data (*28*).

Relative to Viking, the Pathfinder measurements have the following advantages for boundary layer studies. Temperature measurements at several heights allow for a more direct determination of the vertical temperature gradient, and the successful MET sampling strategy has ensured that turbulence and profile data with high temporal resolution (1 Hz or better) are available over a wide variety of conditions, with good systematic coverage of diurnal and interdiurnal variability.

As an example of the analysis of turbulence characteristics from Pathfinder, we show an average temperature power spectrum obtained from the Fourier decomposition of several temperature time series (Fig. 9). Individual spectra are scaled by the appropriate temperature scale T_*, which, following the Monin-Obuchov formulation, is the most important scaling parameter for both vertical profiles and spectra (*28*). The T_* values scaling the spectra were derived from the measured temperature gradients, assuming close to neutral thermal stability due to the proximity of the ground (0.25 m), although T_* ranges from –5 K to +0.2 K. Although simplified, the scaling does a reasonable job in collapsing individual spectra and hence in supporting the applicability of the Monin-Obuchov scaling laws.

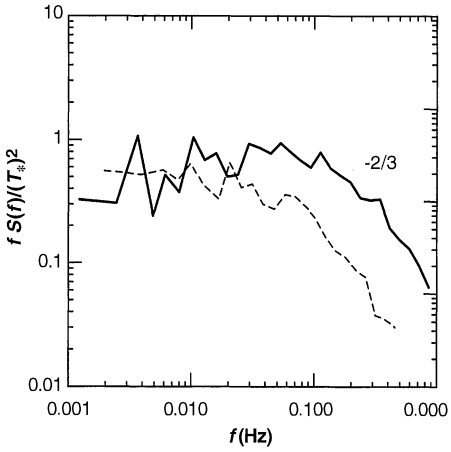

Fig. 9. An average power spectrum $S(f)$ for the martian atmosphere (dashed line) is compared to a similar spectrum from Earth obtained under weakly unstable conditions (bold line). The average spectrum is derived from night- and daytime power spectra for 10-min martian atmosphere temperature time series measured by the bottom mast thermocouple. The spectra are normalized by the turbulence temperature scale T_* derived from the temperature profiles, assuming a logarithmic profile of $T(z) = T_*/\kappa \, \mathrm{Ln}(z/z0)$, where κ is Von Karman's constant and z is altitude, and plotted versus the frequency f. The difference between the Earth and Mars spectra at high frequencies is mainly due to sensor time constants. The line marked 2/3 represents the ideal slope of the inertial subrange power law.

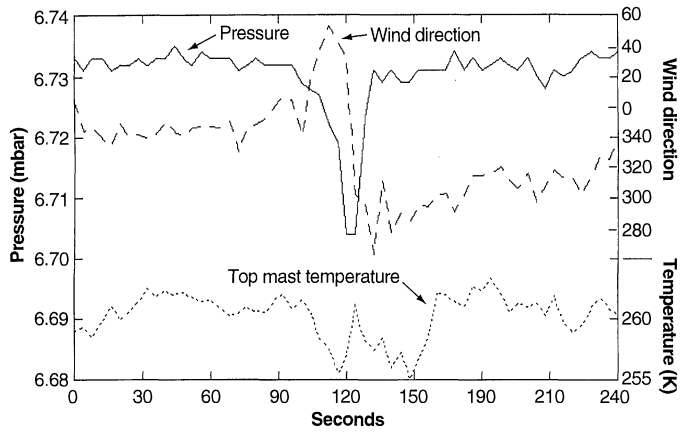

Fig. 8. Pressure, wind, and temperature changes associated with a small-scale vortex, or dust devil, passing through the Pathfinder landing site. The measurements were taken at 4-s intervals.

REFERENCES AND NOTES

1. M. P. Golombek *et al.*, *Science* **278**, 1743 (1997).
2. A. Seiff *et al.*, *J. Geophys. Res* **102**, 4045 (1997).
3. A. Seiff and D. B. Kirk, *ibid.* **82**, 4364 (1977).
4. R. T. Clancy *et al.*, *Icarus* **122**, 36 (1996).
5. S. L. Hess, R. M. Henry, C. B. Leovy, J. A. Ryan, J. E. Tillman, *J. Geophys. Res.* **82**, 4559 (1977).
6. W. M. Folkner, C. F. Yoder, D. N. Yuan, E. M. Standish, R. A. Preston, *Science* **278**, 1749 (1997).
7. W. M. Folkner, personal communication.
8. T. Rivell *et al.*, *J. Spacecr. Rockets* **34**, 265 (1997).
9. P. H. Smith *et al.*, *Science* **278**, 1758 (1997).
10. R. M. Haberle, J. R. Barnes, J. R. Murphy, M. M. Joshi, J. Schaeffer, *J. Geophys. Res.* **102**, 13301 (1997).
11. R. W. Zurek *et al.*, in *Mars*, H. H. Kieffer, B. M. Jakosky, C. W. Snyder, M. S. Matthews, Eds. (Univ. of Arizona Press, Tucson, 1992), pp. 835–933.
12. M. Lopez-Puertas and M. A. Lopez-Valverde, *Icarus* **114**, 113 (1995).
13. P. B. James, H. H. Kieffer, D. A. Paige, in *Mars*, H. H. Kieffer, B. M. Jakosky, C. W. Snyder, M. S. Matthews, Eds. (Univ. of Arizona Press, Tucson, 1992), pp. 934–968.
14. R. T. Clancy, unpublished data.
15. P. J. Gierasch and R. M. Goody, *Planet. Space Sci.* **16**, 615 (1968).
16. R. M. Haberle, H. C. Houben, R. Hertenstein, T. Herdtle, *J. Atmos. Sci.* **50**, 1544 (1993).
17. M. J. Wolff, R. T. Clancy, P. B. James, S. W. Lee, J. F. Bell III, *Bull. Am. Astron. Soc.*, in press.
18. J. A. Magalhães and R. E. Young, *Icarus* **113**, 277 (1995).
19. R. W. Zurek and C. B. Leovy, *Science* **213**, 437 (1981).
20. J. E. Tillman, *J. Geophys. Res.* **93**, 9433 (1988).
21. J. R. Murphy, C. B. Leovy, J. E. Tillman, *ibid.* **95**, 14555 (1990).
22. J. E. Tillman, N. C. Johnson, P. Guttorp, D. B. Percival, *ibid.* **98**, 10963 (1993).
23. R. D. Sharman and J. A. Ryan, *J. Atmos. Sci.* **37**, 1994 (1980).
24. R. J. Wilson and K. Hamilton, *ibid.* **53**, 1290 (1996).
25. B. M. Jakosky, A. P. Zent, R. W. Zurek, *Icarus*, in press.
26. J. A. Ryan and R. D. Lucich, *J. Geophys. Res.* **88**, 11005 (1983).

27. P. Thomas and P. J. Gierasch, *Science* **230**, 175 (1985).
28. J. E. Tillman, L. Landberg, S. E. Larsen, *J. Atmos. Sci.* **51**, 1709 (1994).
29. A. O. Nier and M. B. McElroy, *J. Geophys. Res.* **82**, 4341 (1977).
30. The ASI/MET science team would like to acknowledge the enthusiasm, dedication, and hard work of the engineering teams who built the accelerometer and MET instruments; the Pathfinder spacecraft engineering team who got them to Mars; and the Pathfinder mission operations team who made the instrument do what we wanted and got the data back to Earth. We also thank T. Clancy for supplying unpublished microwave profiles to the ASI/MET team within days of the original observations. The research described in this paper was carried out under contract with NASA.

23 September 1997; accepted 10 November 1997

Results from the Mars Pathfinder Camera

P. H. Smith*, J. F. Bell III, N. T. Bridges, D. T. Britt, L. Gaddis, R. Greeley, H. U. Keller, K. E. Herkenhoff, R. Jaumann, J. R. Johnson, R. L. Kirk, M. Lemmon, J. N. Maki, M. C. Malin, S. L. Murchie, J. Oberst, T. J. Parker, R. J. Reid, R. Sablotny, L. A. Soderblom, C. Stoker, R. Sullivan, N. Thomas, M. G. Tomasko, W. Ward, E. Wegryn

Images of the martian surface returned by the Imager for Mars Pathfinder (IMP) show a complex surface of ridges and troughs covered by rocks that have been transported and modified by fluvial, aeolian, and impact processes. Analysis of the spectral signatures in the scene (at 440- to 1000-nanometer wavelength) reveal three types of rock and four classes of soil. Upward-looking IMP images of the predawn sky show thin, bluish clouds that probably represent water ice forming on local atmospheric haze (opacity ~0.5). Haze particles are about 1 micrometer in radius and the water vapor column abundance is about 10 precipitable micrometers.

After Mars Pathfinder's landing on 4 July 1997, the Imager for Mars Pathfinder (IMP) (*1*) returned the first pictures of Mars from the surface since the Viking missions 21 years before. The panoramic views (Plate 1A) show a terrain littered with boulders stretching to a horizon graced by two hills (the "Twin Peaks"), the southern one conical with a vertical stripe, the northern one broader and banded with possible terraces. But stereoscopic views (Plate 1B) later revealed that the terrain between the lander and the Twin Peaks was a series of shallow gullies, some filled with fines material. This ridge and trough structure appears to be a remnant of the catastrophic floods that came through this area more than 2 billion years ago from Tiu Vallis, southwest to northwest trend, and from Ares Vallis, south-southeast to north-northwest trend.

Here, along with (*2*), we present results on a range of topics from the geomorphology and mineralogy of the site to the atmospheric properties and astronomical observations. During the first 30 days of operation, the IMP returned 9669 images from the surface of Mars; many of these are subframes taken of the sun, various targets on the lander, or multispectral spots on selected rocks and soil. The large panoramas (Plate 1) and their characteristics are listed in Table 1.

Overview of the Pathfinder landing site. The Pathfinder landing site, at the mouth of the Ares and Tiu flood channels, was selected as an area likely to have a diversity of rock types (*3*). As observed from orbit, the principal elements of the geology of the area include (i) relatively smooth plains, (ii) scattered hills that appear to be remnants of a former, eroded surface, (iii) impact crater rims and other ejecta deposits, and (iv) streamlined tails behind topographically prominent features. The southern Chryse plains are pitted by primary and secondary impact craters that indicate a late Hesperian to early Amazonian age. Members of two secondary impact crater clusters lie within 10 km of the lander, toward the southeast and north-northeast. Faint lineaments, trending southwest-northeast, are seen throughout the region following the same trend as the terraced remnants of channels and large tails that occur down slope of the hills. Divergence of these lineaments beyond the mouths of channels reinforces the impression that they are streamlines.

Postflood, geomorphic processes have been relatively benign neither physical nor chemical weathering has led to substantial deterioration of boulders. Derivative debris surrounding rocks is minimal and where debris is collected around boulders, it appears as thin lag deposits atop bright fines, and therefore is interpreted to be aeolian in derivation. Some rocks show indisputable evidence of abrasion, which attests to a flux of saltating particles through the area at some point, although none of the rocks shows the extreme abrasion expected for two or more billion years of exposure to sand blasting at martian wind speeds. At the Viking landing sites, where evidence for abrasion was limited and for sand was disputed, it was suggested that the rocks could have been buried or that windblown particles were incapable of abrasion. Clear evidence of rock abrasion at the Pathfinder site suggests, and may require, sand-transporting winds.

Sight lines to large distant knobs are useful for locating the landing site on the Viking orbiter images; the landing site is about 3 km north-northwest of a 1.5 km diameter impact crater and 1 km east of two hills less than 50 m tall (*3*). Viking orbiter images suggest that a subtle, kilometer-wide asymmetrical rise lies immediately west of the landing site, and that this rise has a short, steep west-northwestern slope and a gentler east-southeastern slope. The twin hills are located along the crest at the western (presumably upstream) end of this ridge. The lander is located on a south-facing slope near the northernmost extension of the rise, close to the point where the relief becomes indistinguishable from the flatter plains. The portion of the rise that extends north of the lander hides all but the summit of a 100 m hill located about 2 km north of the lander.

The Pathfinder site is more rugged than either of the Viking landing sites (*4*) and has a pronounced ridge-and-trough texture (Plates 2 and 4). Over distances of 50 to 100 m, these ridges and troughs have amplitudes as high as 5 m, and are irregularly spaced but commonly 15 to 25 m crest-to-crest. Southwest-northeast and south-north trends comparable with the large-scale Tiu and Ares flow directions are modestly ex-

P. H. Smith, D. T. Britt, M. Lemmon, R. J. Reid, M. G. Tomasko, E. Wegryn, Lunar and Planetary Laboratory, University of Arizona, Tucson, AZ 85721, USA.
J. F. Bell III and R. Sullivan, Cornell University, Ithaca , NY 14853, USA.
N. T. Bridges, K. E. Herkenhoff, J. N. Maki, T. J. Parker, Jet Propulsion Laboratory, California Institute of Technology, Pasadena, CA 91109, USA.
L. Gaddis, J. R. Johnson, R. L. Kirk, L. A. Soderblom, W. Ward, U.S. Geological Survey, Flagstaff, AZ 86001, USA.
R. Greeley, Arizona State University, Tempe, AZ 85287, USA.
H. U. Keller, R. Sablotny, N. Thomas, Max Planck Institute for Aeronomy, Kathenburg–Lindau, Germany.
R. Jaumann and J. Oberst, DLR, Berlin, Germany.
M. C. Malin, Malin Space Science Systems, San Diego, CA 92191, USA.
S. L. Murchie, Applied Physics Laboratory, Johns Hopkins University, Baltimore, MD 21218, USA.
C. Stoker, NASA Ames Research Center, Moffett Field, CA 94035, USA.

* To whom correspondence should be addressed. E-mail: psmith@lpl.arizona.edu